Iron Oxide/Gold Core/Shell Nanoparticles for Ultrasensitive Detection of Carbohydrate–Protein Interactions

ARTICLE *in* ANALYTICAL CHEMISTRY · SEPTEMBER 2009

Impact Factor: 5.64 · DOI: 10.1021/ac9012286 · Source: PubMed

Anal. Chem. **2009,** *81,* 7750–7756

Iron Oxide/Gold Core/Shell Nanoparticles for Ultrasensitive Detection of Carbohydrate–Protein Interactions

Chi-Hui Liang,[†] Cheng-Chi Wang,[‡] Yu-Chen Lin,[§] Chung-Hsuan Chen,[†] Chi-Huey Wong,*[,†,‡,§] and Chung-Yi Wu*[,†]

The Genomics Research Center, Academia Sinica, Taipei, 115 Taiwan, and Institute of Biochemical Science and Department of Chemistry, National Taiwan University, Taipei, 106 Taiwan

Changes in the expression of cell surface glycan are often associated with malignant metastasis. The expression level may be dramatically enhanced during tumor progression. A highly sensitive assay that is capable of detecting low levels of cancer-associated carbohydrate antigens can be a powerful tool for early diagnosis. In this work, an ultrasensitive glycans array using iron oxide/gold core/shell nanoparticles conjugated with antibodies or proteins is developed. A magnetic field is applied to quickly bring nanoparticle labeled proteins or antibodies from a solution to an array of carbohydrates immobilized on glass slides and to help them to encounter the carbohydrates at very low concentration. The gold shell provides a well established platform for conjugation of biomolecules. Well-defined recognition systems, namely, mannose derivatives (Man1, Man4, and Man9) with a mannose binding lectin (Concanavalin A) and a stage-specific embryonic antigens-3 (SSEA-3) with a monoclonal antibody (anti-SSEA-3) were chosen to establish this detection tool. Array systems were conducted to determine their surface dissociation constant ($K_{D,surface}$) and their binding specificity for qualitative and quantitative analysis of carbohydrate–protein and carbohydrate–antibody interactions. When coupled with a signal amplification method based on nanoparticle-promoted reduction of silver, the sensitivity of an iron oxide/gold core/shell nanoparticle-based assay reached to sub-attomole level in carbohydrate detection.

Glycosylation is the process of adding saccharides to proteins and lipids. It plays important roles in a wide variety of biological processes including bacterial pathogenesis, inflammation, and cancer cell metastasis.[1,2] Regarding cancer, some of the most important processes leading to malignant transformation are alterations in glycosylation levels or patterns on the cell surface.[3,4] Several cancer-associated glycans have been identified as mediating key pathophysiological events during the various steps of cancer progression. For example, it is recommended that the capping monosaccharide sialic acid has a high metastatic ability in many types of cancers.[5] The amount of sialic acid present on the surface of the malignant cells has been correlated directly with metastasis progression. Terminal glycan epitopes including sialyl Lewis x, Lewis y, and Globo H are usually found on transformed cells.[6,7] Thus, the glycosylation pattern and glycosylation levels of cells essentially often act as biomarkers to convey information about the physiological state of the cells.

An ultrasensitive and simple method for detecting and quantifying biomarkers is crucial for early detection of diseases. Recent clinical studies have indicated some biomarker concentrations are below the detection limit of diagnostic immunoassay technologies; therefore, more-sensitive detection is required for earlier detection of certain diseases. Examples of immunochemical tests for cancer-associated carbohydrate biomarkers, which include carbohydrate antigen (CA) 125, carbohydrate antigen (CA) 15-3, or carbohydrate antigen (CA) 19-9, are antibody-based assays for glycosylated proteins often associated with ovarian, breast, or other cancer types.[8,9] These tests are not specific or sensitive enough for early cancer detection and, therefore, are not recommended by the American Society of Clinical Oncology. Recently, Wang et al. suggested that a glycan array provides a new tool for possible early stages of breast cancer diagnosis.[10] This array method reaches an attomole of glycan–antibody detection limit and is 5 orders of magnitude more sensitive than the traditional ELISA (enzyme-linked immunosorbent assay) method.[2,10] In addition, the most important advantage of a glycan array is that it can effectively mimic the presentation of glycans on the surface of malignant cells to exhibit multivalent interactions with receptors. Therefore,

* To whom correspondence should be addressed. E-mail: chwong@gate.sinica.edu.tw (C.-H.W.) and cyiwu@gate.sinica.edu.tw (C.-Y.W.).
† Academia Sinica.
‡ Institute of Biochemical Science, National Taiwan University.
§ Department of Chemistry, National Taiwan University.

(1) Varki, A.; Cummings, R.; Esko, J. D.; Freeze, H.; Hart, G. W.; Marth, J. *Essentials of Glycobiology*; Cold Spring Harbor Press: New York, 1999.
(2) (a) Liang, P. H.; Wu, C. Y.; Greenberg, W. A.; Wong, C. H. *Curr. Opin. Chem. Biol.* **2008**, *12*, 86–92. (b) Wu, C. Y.; Liang, P. H.; Wong, C. H. *Org. Biomol. Chem.* **2009**, *7*, 2247–2254.
(3) Meezan, E.; Wu, H. C.; Black, P. H.; Robbins, P. W. *Biochemistry* **1969**, *8*, 2518–2524.
(4) Dube, D. H.; Bertozzi, C. R. *Nat. Rev. Drug Discovery* **2005**, *4*, 477–488.
(5) Schauer, R. *Trends Biochem. Sci.* **1985**, *10*, 357–360.
(6) Sell, S. *Hum. Pathol.* **1990**, *21*, 1003–1019.
(7) Taylorpapadimitriou, J.; Epenetos, A. A. *Trends Biotechnol.* **1994**, *12*, 227–233.
(8) Suzuki, K.; Muraishi, O.; Tokue, A. *J. Urol.* **2002**, *167*, 16–20.
(9) Porcel, J. M.; Vives, M.; Esquerda, A.; Salud, A.; Perez, B.; Rodriguez-Panadero, F. *Chest* **2004**, *126*, 1757–1763.
(10) Wang, C. C.; Huang, Y. L.; Ren, C. T.; Lin, C. W.; Hung, J. T.; Yu, J. C.; Yu, A. L.; Wu, C. Y.; Wong, C. H. *Proc. Nat. Acad. Sci. U.S.A.* **2008**, *105*, 11661–11666.

10.1021/ac9012286 CCC: $40.75
Published on Web 08/18/2009

it provides a more appropriate way to study protein−carbohydrate interactions than ELISA analysis.[11] However, microarray techniques including DNA,[12] protein,[13] and carbohydrate[14] mainly rely on the use of fluorescent molecular dye labels which have to overcome several drawbacks, such as quenching phenomena and photochemical instability.[15,16] Instead, nanoparticle-based assays have attracted both fundamental and practical interest in medical diagnostics.[17,18] The unique optical, electronic, and magnetic properties of nanoparticles have led to tremendous progress in biomolecular detection assays.[19] Mirkin and co-workers have developed a scanometric DNA array system coupled with a signal enhancement method based on the precipitation of silver on gold nanoparticle tags.[16] The sensitivity of this scanometric array detection system exceeds that of the analogous fluorophore system by 2 orders of magnitude. Using similar principles, gold nanoparticles have been applied in ultrasensitive detection of DNA hybridization, protein−protein interactions, and carbohydrate−protein interactions.[20−23] Particularly, attraction is the development of the multiplexed biobarcode assay which has given the lowest detection limit to date for both nucleic acid (zeptomolar) and protein targets (attomolar).[24] The excellent analytical sensitivity of this approach can be attributed to two type of particles (magnetic particles and gold nanoparticles) to accomplish sample purification, amplification and detection. With the use of the biobarcode assay, researchers and clinicians have opportunities to apply new biomarkers for detection of many types of diseases with conventional technology.

Inspired by the concept of the biobarcode assay, we introduce iron oxide/gold core/shell nanoparticles as a means to increase complexity and functionality in a scanometric array detection system. Core/shell nanoparticles consist of discrete domains of different materials and, thus, can exhibit the properties of different components in the same structure. Here, iron oxide/gold core/shell nanoparticles combine the ability of magnetic property for enrichment, surface modification, and signal enhancement in a single entity. This powerful combination enables us to quickly concentrate target biomolecules by an external magnetic field and amplify signal by depositing silver on the gold surface of core/shell nanoparticles. Qualitative and quantitative analysis of carbohydrate−protein and carbohydrate−antibody interactions are conducted by this core/shell nanoparticle-based assay to determine the surface dissociation constant ($K_{D,surface}$) and binding specificity. The sensitivity of this core/shell nanoparticle-based assay can reach the subattomole limit of carbohydrate detection. It should be noted that assessing carbohydrate−protein or carbohydrate−antibody interactions are usually difficult due to weak affinities and limited sources of structurally complex carbohydrates. The ability to identify a very low concentration of cancer-associated carbohydrate antigens by this core/shell nanoparticle-based assay without any costly or complex instrumentation would be a very powerful tool for point-of-care diagnostics and even allow for the large-scale screening of particular diseases prior to more costly and invasive procedures.

EXPERIMENTAL SECTION

Materials. Concanavalin A (Con A), bovine serum albumin (BSA), hydrogen tetrachloroaureate (III) trihydrate ($HAuCl_4$), sodium hydroxide, iron(II) chloride tetrahydrate 97%, iron(III) chloride hexahydrate 99%, sodium citrate, potassium carbonate (K_2CO_3), D-glucose, polyethylene glycol (PEG; MW = 20 000), sodium chloride, and acetic acid were obtained from Sigma-Aldrich (St. Louis, MO). Sodium hydroxide (NaOH) and hydroxylamine were purchased from Merck (Darmstadt, Germany). All chemicals used were analytical grade and used as received. *N*-Hydroxysuccinimide coated glass slides were purchased from Nexterion Slide H (SCHOTT North America). Antibodies were antihuman/mouse SSEA-3 (stage-specific embryonic antigen-3) (eBioscience). Water was purified by Milli-Q ultrapure water systems. The NdFeB magnet, purchased locally (Taiwan Magnetic Corp. Ltd., Taipei), was used to preconcentrate nanoparticle labeled proteins or antibodies. Buffers used in the experiment include the print buffer (pH 8.5, 300 mM phosphate buffer containing 0.005% (v/v) Tween 20), the blocking buffer (50 mM ethanolamine in 50 mM sodium borate buffer pH 9.0), and the washing buffer (PBST buffer; PBS and 0.05% Tween 20). Print buffer and blocking buffer were prepared freshly before use. The Globo H and its analogs were prepared according to the previous one-pot programmable protocol.[25] Mannose derivatives (Man1, Man4, and Man9) were synthesized as previously described.[26]

Synthesis of Iron Oxide/Gold Core/Shell Nanoparticles. The preparation of gold coated iron oxide nanoparticles involved an initial synthesis of iron oxide nanoparticles as seeds and a subsequent reduction of Au(III) in the presence of the seeds. Briefly, the iron oxide nanoparticles were prepared by coprecipitation of Fe(II) and Fe(III) chlorides with 1.5 M NaOH as the

(11) Mammen, M.; Choi, S. K.; Whitesides, G. M. *Angew. Chem., Int. Ed.* **1998**, *37*, 2755–2794.
(12) (a) Ramsay, G. *Nat. Biotechnol.* **1998**, *16*, 40–44. (b) Heller, M. J. *Annu. Rev. Biomed. Eng.* **2002**, *4*, 129–153.
(13) (a) Zhu, H.; Snyder, M. *Curr. Opin. Chem. Biol.* **2003**, *7*, 55–63. (b) Templin, M. F.; Stoll, D.; Schrenk, M.; Traub, P. C.; Vohringer, C. F.; Joos, T. O. *Trends Biotechnol.* **2002**, *20*, 160–166.
(14) (a) Park, S.; Shin, I. *Angew. Chem., Int. Ed.* **2002**, *41*, 3180–3182. (b) House, B. T.; Mrksich, M. *Chem. Biol.* **2002**, *9*, 443–454. (c) Wang, D.; Liu, S.; Trummer, B. J.; Deng, C.; Wang, A. *Nat. Biotechnol.* **2002**, *20*, 275–281. (d) Kukui, S.; Feizi, T.; Galustian, C.; Lawson, A. M.; Chai, W. *Nat. Biotechnol.* **2002**, *20*, 1011–1017. (e) Love, K. R.; Seeberger, P. H. *Angew. Chem., Int. Ed.* **2002**, *41*, 3583–3586. (f) Mellet, C. O.; Garciá Fernández, J. M. *ChemBioChem* **2002**, *2*, 819–822. (g) Paulson, J. C.; Blixt, O.; Collins, B. E. *Nat. Chem. Biol.* **2007**, *2*, 238–248. (h) Feizi, T.; Fazio, F.; Chai, W.; Wong, C. H. *Curr. Opin. Struct. Biol.* **2003**, *13*, 637–645.
(15) (a) Schweitzer, B.; Wiltshire, S.; Lambert, J.; O'Malley, S.; Kukanskis, K.; Zhu, Z.; Kingsmore, S. F.; Lizardi, P. M.; Ward, D. C. *Proc. Natl. Acad. Sci. U.S.A.* **2000**, *97*, 10113–10119. (b) Kodadek, T. *Chem. Biol.* **2001**, *8*, 105–115.
(16) Taton, T. A.; Mirkin, C. A.; Letsinger, R. L. *Science* **2000**, *289*, 1757–1760.
(17) Alivisatos, P. *Nat. Biotechnol.* **2004**, *22*, 47–52.
(18) Parak, W. J.; Gerion, D.; Pellegrino, T.; Zanchet, D.; Micheel, C.; Williams, S. C.; Boudreau, R.; Le Gros, M. A.; Larabell, C. A.; Alivisatos, A. P. *Nanotechnology* **2003**, *14*, R15–R27.
(19) Rosi, N. L.; Mirkin, C. A. *Chem. Rev.* **2005**, *105*, 1547–1562.
(20) Wang, Z. X.; Lee, J.; Cossins, A. R.; Brust, M. *Anal. Chem.* **2005**, *77*, 5770–5774.
(21) Hou, S. Y.; Chen, H. K.; Cheng, H. C.; Huang, C. Y. *Anal. Chem.* **2007**, *79*, 980–985.
(22) Gao, J. Q.; Liu, D. J.; Wang, Z. X. *Anal. Chem.* **2008**, *80*, 8822–8827.
(23) Guarise, C.; Pasquato, L.; De Filippis, V.; Scrimin, P. *Proc. Nat. Acad. Sci. U.S.A.* **2006**, *103*, 3978–3982.
(24) Nam, J. M.; Thaxton, C. S.; Mirkin, C. A. *Science* **2003**, *301*, 1884–1886.
(25) Huang, C. Y.; Thayer, D. A.; Chang, A. Y.; Best, M. D.; Hoffmann, J.; Head, S.; Wong, C. H. *Proc. Nat. Acad. Sci. U.S.A.* **2006**, *103*, 15–20.
(26) Lee, H. K.; Scanlan, C. N.; Huang, C. Y.; Chang, A. Y.; Calarese, D. A.; Dwek, R. A.; Rudd, P. M.; Burton, D. R.; Wilson, I. A.; Wong, C. H. *Angew. Chem., Int. Ed.* **2004**, *43*, 1000–1003.

reductant.[27] The black precipitate was collected on a magnet, followed by washing with water several times. The iron oxide nanoparticles were then stirred with an equal volume of 0.1 M sodium citrate overnight to exchange adsorbed OH^- with citrate anions. The iron oxide/citrate nanoparticles were isolated by centrifugation and redispersed in a 0.01 M glucose solution. The iron oxide/citrate nanoparticles were diluted to 1 mM in 0.1 M glucose, and aliquots of 1% $HAuCl_4$ were dropwisely added along with an excess of 0.01 M hydroxylamine which promotes Au^{3+} surface catalyzed reduction, rather than Au particle nucleation.[28] As the particles were gradually coated by gold, the black iron oxide particles turn reddish brown. These gold coated iron oxide particles were separated out from the solutions by a magnetic field. Details of the core/shell nanoparticle characterizations are available in the Supporting Information.

Labeling of Concanavalin A with Iron Oxide/Gold Core/Shell Nanoparticles. Adsorption of proteins to iron oxide/gold core/shell nanoparticle is not only pH dependent but also closely related to the ionic strength.[29] The stability of the iron oxide/gold core/shell nanoparticle was maintained by electrostatic repulsion. When electrolytes were added to nanoparticles, cohesion of the particles occurs and results in flocculation unless stabilized by the adsorption of a protecting substance, such as protein.[30] In order to provide optimal conditions for the iron oxide/gold nanoparticle−Con A complex formation, the ionic concentration of Con A solutions must be very low. But, the solubility of the Con A was low in distilled water. Therefore, Con A should be dissolved in very dilute salt solutions prior to complex formation. The influence of ionic strength on the nanoparticle−Con A complex was studied in NaCl solutions of various ionic strengths. Details were available in the Supporting Information. Results showed that Con A against 0.01 M NaC1 has produced a stable nanoparticle−protein complex indicating that low concentrations of NaCl may be tolerated. In the nanoparticle labeling Con A experiment, the molecular weight of Con A is 96 000, and the ionic strength during the binding process is kept below 0.01 M. In addition, the maximal adsorption of proteins to the iron oxide/gold core/shell nanoparticle occurred at pH values close to or slightly basic to the isoelectric point of a given protein. Thus, depending on the isoelectric point of a protein, the pH of the iron oxide/gold core/shell nanoparticle solution must be adjusted either by addition of 0.2 M K_2CO_3 or by addition of 1 M acetic acid to increase or decrease the pH value. In this study, the iron oxide/gold core/shell nanoparticle used was adjusted to pH 8 for the Concanavalin A labeling purpose. To check the pH of iron oxide/gold core/shell nanoparticles, two drops of 1% polyethylene glycol (PEG) MW 20 000 were added to 10 mL of iron oxide/gold core/shell nanoparticle solution to stabilize it before the pH electrode was inserted. One milliliter of the Concanavalin A solution (2 mg/mL) was added to 10 mL of iron oxide/gold core/shell nanoparticles with a Pasteur pipet and mixed rapidly. The Concanavalin A and iron oxide/gold core/shell nanoparticles were then allowed to mix for 10 min. The mixture is further stabilized by the addition of 0.5 mL of 1% aqueous PEG 20000. The resulting complex was centrifuged to remove the excess of unbound Concanavalin A. The core/shell nanoparticle-Concanavalin A complex was centrifuged at 1500 rpm for 20 min to remove any large aggregates and then centrifuged in 50 mL centrifuge tubes at 14 000 rpm for 30 min. The colorless supernatant was aspirated and discarded leaving a dark-red pool which corresponds to the iron oxide/gold nanoparticle labeled Concanavalin A. BSA (100 μL of 10%) was added into the iron oxide/gold core/shell nanoparticle-labeled Concanavalin A to block any unbound active site on the iron oxide/gold nanoparticle surface. After 1 h of blocking at 4 °C, the preparation was centrifuged at 8000 rpm for 30 min. The dark-red pool was recovered in 1 mL of 0.1 M phosphate-buffered saline (PBS) with a pH of 7.4 and stored at 4 °C for further use.

Labeling of Antihuman/Mouse SSEA-3 with Iron Oxide/Gold Core/Shell Nanoparticles. Conjugation of antibodies to iron oxide/gold core/shell nanoparticles depended upon three separate but dependent phenomena which are ionic strength, hydrophobic attraction, and covalent binding between the gold and sulfur atoms. As the ionic strength increased, the electrostatic repulsion between liked-charged materials reduced and electrostatic attraction between oppositely charged materials decreased, which was expected on the basis of DLVO theory.[31] The ionic strength increase was also responsible for a reduction of the thickness of the electric double layer over charged surfaces which governs a decrease in electrostatic interaction between antibodies and nanoparticles, and compression of the electrical double layer was usually accompanied by coagulation. Therefore, the ionic strength of antibodies should be kept as low as possible when the nanoparticle is adsorbed by electrostatic attraction.[32] Hydrophobic attraction and covalent binding were also essential in antibody−nanoparticle conjugation. The nanoparticles can attach to an amino acid of the antibodies by lysing (charge attraction) tryptophan (hydrophobic attraction), cysteine (sulfur binding), or methionine (sulfur binding). Generally speaking, the strongest covalent binding occurred at the sulfur hinge region, which is at the opposite end from the antigen binding site of the Fab′, so the nanoparticle does not interfere with antibody binding and native immune reactivity is preserved.[33] In order to form a strong absorption of antibody onto the nanoparticle surface, a preliminary titration was performed to determine the optimum conditions for conjugation. Briefly, a solution of iron oxide/gold core/shell nanoparticles was adjusted to pH 10 with K_2CO_3, and 50 μL was pipetted into Eppendorf tubes. The antihuman/mouse SSEA-3 antibody was added to each tube in a series from 0 to 40 μL in steps of 0, 10, 20, 30, and 40. The volume in each tube was made up to 200 μL by adding PBS (pH 7.4). Sodium chloride (50 μL of 10%) was added to each tube, and the minimum amount of antibody required to stabilize the iron oxide/gold core/shell nanoparticle solution was indicated by the amount in which no precipitation occurs upon the addition of NaCl.

(27) Kouassi, G. K.; Irudayaraj, J. *Anal. Chem.* **2006**, *78*, 3234–3241.
(28) Lyon, J. L.; Fleming, D. A.; Stone, M. B.; Schiffer, P.; Williams, M. E. *Nano Lett.* **2004**, *4*, 719–723.
(29) Roth, J. *J. Histochem. Cytochem.* **1983**, *31*, 987–999.
(30) Geoghegan, W. D.; Ackerman, G. A. *J. Histochem. Cytochem.* **1977**, *25*, 1187–1200.
(31) (a) Lyklema, J. *Fundamentals of Interface and Colloid Science*; Academic Press: London, 1995. (b) Verwey, E. J. W.; Overbeek, J.; Th., G. *Theory of the Stability of Lyophobic Colloids*; Elsevier: New York, 1948.
(32) Hainfeld, J. F.; Powell, R. D. *J. Histochem. Cytochem.* **2000**, *48*, 471–480.
(33) Hainfeld, J. F. *Science* **1987**, *236*, 450–453.

To conjugate antibodies on iron oxide/gold core/shell nanoparticles, 30 μL of antihuman/mouse SSEA-3 antibody was added to the 50 μL of the iron oxide/gold core/shell nanoparticle solution (pH 10) with gentle agitation. This amount of antibody was 50% more than the minimum amount (determined according to the preliminary titration) for coating the unmodified portion of the iron oxide/gold nanoparticle surface. The mixture was incubated at 4 °C overnight. Upon centrifugation at 8000 rpm for 30 min at 4 °C, a clear supernatant of unbound antibody and a dark-red, loosely packed sediment of the iron oxide/gold core/shell nanoparticle-labeled antibodies were obtained. Occasionally, black sediment of iron oxide/gold nanoparticles was also found; this sediment was attributed to aggregation of iron oxide/gold nanoparticle that was not effectively stabilized by the antibody coating. Next, the clear supernatant and black sediment were discarded, and the loosely packed iron oxide/gold core/shell nanoparticle-labeled antibody sediment was resuspended in 1 mL of PBS buffer (10 mM, pH 7.4). A 100 μL of 10% BSA was added into the iron oxide/gold core/shell nanoparticle-labeled antibody solution to block any unbound active site on the iron oxide/gold nanoparticle surface. After 1 h of blocking at 4 °C, the preparation was centrifuged at 8000 rpm for 30 min. The loose precipitate was finally resuspended in 2 mM PBS buffer, pH 7.4 containing 0.1% BSA for further use.

Glycan Array Fabrication. Amino-reactive *N*-hydroxysuccinimide (NHS)-activated glass microscope slides were used to fabricate glycan arrays by the standard protocol of Protein Application Nexterion Slide H. The NHS groups on the glass surface react readily with the primary amines of the amino modified glycans to form an amide linkage. Amine-modified glycans with desired concentration were dissolved in printing buffer (pH 8.5, 300 mM phosphate buffer with 0.005% (v/v) Tween 20) and were spotted on the glass microscope slides by robotic pin (BioDot, Cartesian Technologies; SMP3, Telehem International) deposition. Print slides were incubated under 80% humidity at 37 °C for 2 h followed by desiccation overnight. Before the binding assay, print slides were immersed with blocking buffer (50 mM ethanolamine in 50 mM borate buffer, pH 9.2) at room temperature for 1 h to remove remaining free NHS groups and then washed with washing buffer (PBST; 50 mM PBS buffer with 0.05% (v/v) Tween 20, pH 7.4) and DI water several times. These slides were dried by argon flow and stored at room temperature in a vacuum desiccator until use.

To test the limit of detection, NHS-coated glass slides were printed with Man1 with 13 concentrations ranging from 10^{-7} to 10^{-19} mol with two replicates, which were arranged in a 13 × 2 pattern and yielded spots of ~1 mm in diameter. To determine the $K_{D,surface}$, the slides of Man1, Man4, and Man9 were printed with a concentration of 1 mM. After 1 day of reaction, the slides were washed with PBST buffer (0.05% Tween 20) for 30 min and then blocked with blocking buffer for another hour. The slides were dried by purging with argon gas and then stored at room temperature in a vacuum desiccator. The slides were washed with PBS buffer (pH 7.4) before use.

Concanavalin A Binding Assay. Iron oxide/gold nanoparticle-labeled Concanavalin A was diluted to the desired concentration with 10 mL of probe buffer (10 mM PBS and 1% BSA (w/w)). A 200 μL volume of iron oxide/gold nanoparticle-labeled Concanavalin A was added and spread throughout the slide at fixed concentrations in the sensitivity experiment or at the various concentrations in determining surface dissociation constants of carbohydrates. A NdFeB magnet was placed beneath the slide for attracting nanoparticle-labeled Con A. Incubation was performed with shaking and magnetic attraction for 1 h at 25 °C. The slide was subsequently washed three times each with washing buffer (pH 7.4), PBS buffer (pH 7.4), and Milli-Q ultrapure water and dried under argon flow.

Antibody Binding Assay. The antibody binding assay was conducted similarly to the Concanavalin A binding assay. Briefly, the iron oxide/gold nanoparticle-labeled antihuman/mouse SSEA-3 antibodies were prepared in 10 mM PBS buffer (pH 7.4, containing 1% BSA) and added to the slide. A magnet was applied as described above. In each case, 200 μL of iron oxide/gold nanoparticle-labeled antihuman/mouse SSEA-3 solution was pipetted onto the printed carbohydrate (Globo H and its analogs) substrate and allowed to react. After incubation in a humidifying chamber with shaking and magnetic attraction for 1 h, the slides were washed and dried by following the standard procedure.

Silver Enhancement Method. To assist visualization of carbohydrate−antibody or carbohydrate−lectin hybridization at very low concentration, silver enhancement reagents were used to amplify the signal of the iron oxide/gold core/shell nanoparticles. This process increased the scanned intensity by a factor as large as 10^5.[16] The above tested slides were soaked in silver enhancer solution for 15 min at 4 °C and fixed by the addition of 2.5% sodium thiosulfate for 3 min at room temperature. After signal amplification by silver deposition, the slides were detected with a simple flatbed scanner (Perfection V500 PHOTO, Epson).

Data Analysis. The intensity of each dot was quantified by the Quality One software program (Bio-Rad). The local background originating from the slide was recorded and subtracted from each image prior to evaluation. Equilibrium binding data were analyzed by nonlinear curve fitting of the Langmuir binding isotherms using the OriginLab software. The mean value and standard deviation of the signal were determined for all data points collected.

RESULTS AND DISCUSSION

To realize the benefits of high-specificity and high-sensitivity detection coupled with multiple labeling capabilities, we designed multifunctional nanoparticle probes that can be used for carbohydrate detection. These probes consist of 30 nm diameter iron oxide/gold core/shell nanoparticles functionalized with protein or antibody. The binding scheme and detection rationale employed was schematically shown in Figure 1.

Specificities of Carbohydrate−Antibody Interaction. To detect specific carbohydrate−antibody interactions on the glycan array, the antibody was conjugated with nanoparticles and Globo H and its analogs were synthesized. Eight different carbohydrates, Globo H, and truncated structures (Figure 2a), were spotted on the slide to be probed with antihuman/mouse SSEA-3 monoclonal antibody, which were chosen to compare with our previous results.[10] The array was printed with these carbohydrates in an 80 μM concentration with three replicates, which were designed in a 3 (columns) × 8 (rows) pattern. The slide was subsequently

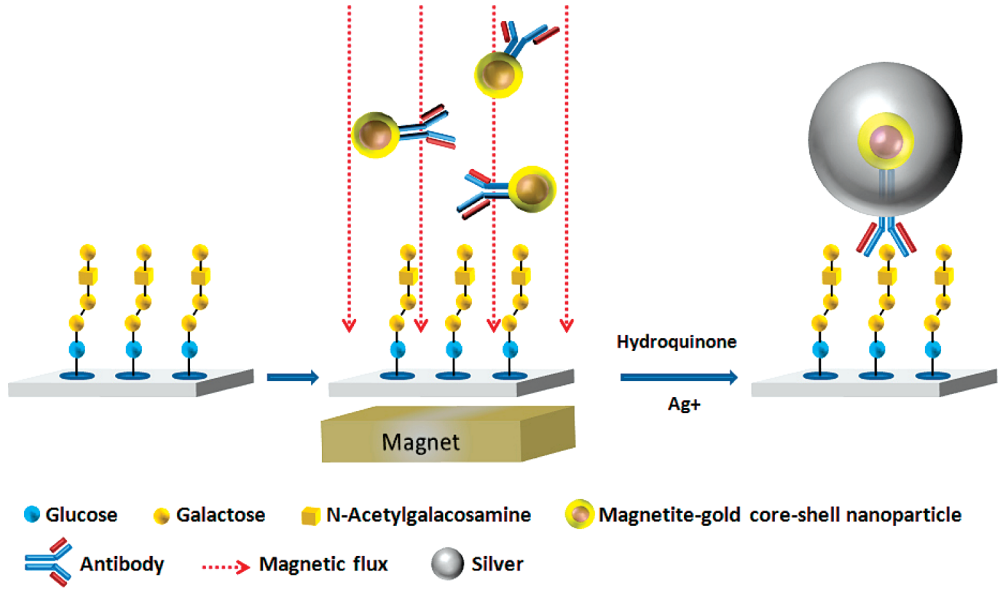

Figure 1. Schematic description of iron oxide/gold core/shell nanoparticle-based assays (from left to right): the binding of core/shell nanoparticle-labeled antibodies to the spotted tumor associated carbohydrate antigen (SSEA-3), then applying magnetic fields to quickly bring nanoparticle-labeled antibodies from a solution to encounter the carbohydrates (SSEA-3) at very low concentration, followed by the silver enhancement step and reading by a conventional flatbed scanner.

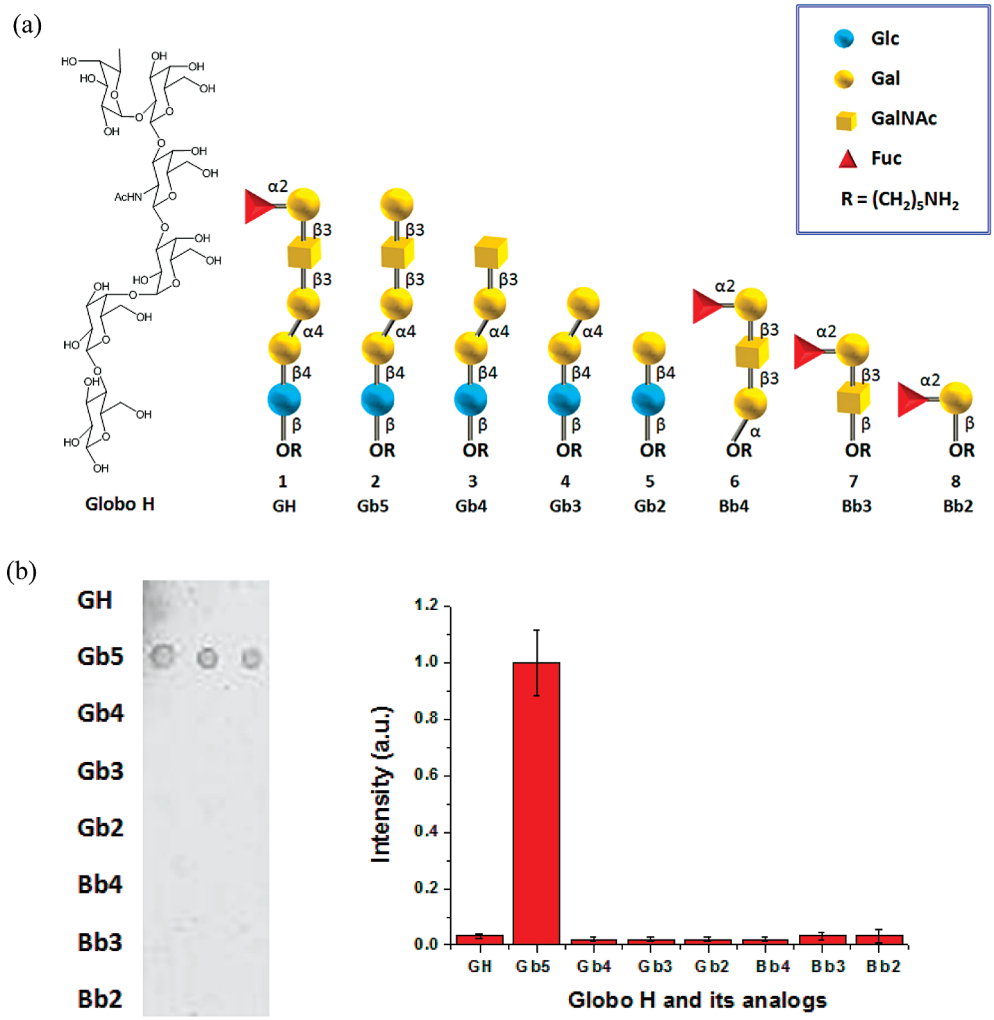

Figure 2. (a) Chemical structure of Globo H and truncated derivatives. (b) A scanometric image and corresponding analysis of glycan array after probing with iron oxide/gold nanoparticle-labeled anti-SSEA-3 antibody and enhancement by silver deposition. The slide contained Globo H analogs 1−8 printed at an 80 μM concentration, and each row contained three replicate spots.

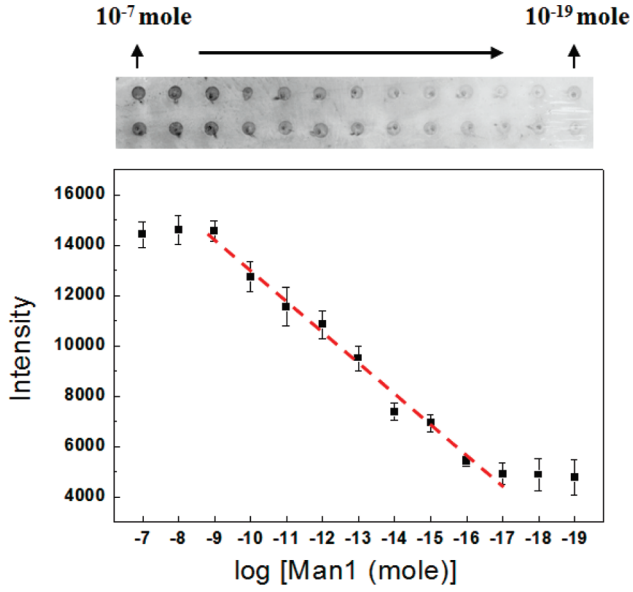

Figure 3. Sensitivity of iron oxide/gold nanoparticle-based assays. NHS-coated glass slides were printed with Man1 with 13 concentrations ranging from 10^{-7} to 10^{-19} mol with two replicates, which were arranged in a 13 × 2 pattern. A slide image was obtained from a flatbed scanner after a lectin incubation assay with Con A. A corresponding plot of intensity versus the concentrations of Man1 showed the linear working range from 10^{-9} to 10^{-16} mol. The detection limit was determined to be at 100 fM printing concentration and subattomole quantities of carbohydrates per spot. The arrow refers to the printing concentration.

incubated with iron oxide/gold nanoparticle-labeled antihuman/mouse SSEA-3 antibodies (~10 nM) and placed under a magnetic field. After silver enhancement, the slide which exhibited gray spots visible to the naked eye could be imaged with a flatbed scanner (Figure 2b). These results demonstrate that the antihuman/mouse SSEA-3 recognized Gb5 (SSEA-3 antigen) specifically without any cross-reactivity to other Globo H analogs which was consistent with our previous fluorescence assays.[10] More importantly, iron oxide/gold nanoparticle-labeled antibodies retained their binding specificity, confirming their potential in disease detection.

Sensitivity of Carbohydrate−Lectin Interaction. The sensitivity of this method was examined by varying the concentrations of monomannose derivative (bearing primary amine Man1) in the spotting solution while keeping the concentrations of lectins constant. Man1 was printed on the glass slide in concentrations ranging from 100 mM to 100 fM (Figure 3) and incubated with nanoparticle-labeled Concanavalin A (1 μM). To decrease the limit of detection, magnetic attraction and silver enhancement were applied. In principle, even an ultimate detector capable of detecting a single molecule cannot have a limit of detection much lower than a femtomole because of the impractically long time needed for a molecule to encounter the reactor. To further decrease the limit of detection while accelerating the assay, passive diffusion of analytes was replaced by their active delivery with an external magnetic force. The limit of detection in such active assays was found to be in the 100 zeptomole printing concentration (1 μL spotting volume), when the ratio of signal-to-noise was more than ten. To determine the linear ranges of the plot shown in Figure 3, the range of concentrations that best fitted the linear equation $y = ax + b$ were specified. The relationship between glycan concentration in an array spot and spot intensity reported by a scanner was linear only within a certain range of intensities, being dominated by saturation above that range. As shown in Figure 3, the glycan spot signal increased linearly with the logarithm of the mannose concentration from 10^{-9} to 10^{-16} mol and began to saturate above 10^{-9} mol. The equation for the linear fit was relative intensity = 1250 × log [Man 1(mol)] + 25505 and the correlation coefficient (r^2) of the data was 0.98.

The corresponding fluorescence assay with nanomolar (attomole) detection limits was reported by Liang et al.[34] Compared to the fluorescent method, the iron oxide/gold nanoparticle-based assay substantially overcame the drawback of photoinstability and still yielded a sensitivity that was an order of magnitude greater than the cited fluorescence array sensitivity on the same target under near identical conditions. These results indicated that an iron oxide/gold nanoparticle-based assay could be useful in ultrasensitive detection and quantitative analysis of tumor-associated glycan biomarkers and could have great potential in early diagnosis of cancer by labeling glycan biomarkers on tumor cell surface.[35] Strategies for the early detection of cancer by accumulation of the simple sugar 2-fluoro-2-deoxy-glucose (FDG) in tumor tissue relative to healthy tissue have been demonstrated by Gambhir.[36] Advantages of the use of our developed methods are mimicking the cell surface glycan in a manner of multivalent interaction and the possibility to identify tumor associated glycan in a very sensitive way. In fact, the real world samples of glycans on the cell surface are more complex and may not constitute by pure glycan. This will result in decreasing array sensitivity or even array specificity. Further studies in the glycan mixture array are progressing in our lab.

Determination of Surface Dissociation Constants. The dissociation constant (K_D) is a useful quantitative parameter to describe the strength of binding or affinity between the ligands and the receptors (carbohydrate−protein). In order to further determine the surface dissociation constant ($K_{D,surface}$) for surface-coated mannose derivatives with mannose binding lectins, Concanavalin A and glycan arrays (Man1, Man4, and Man9; see Figure 4a) were incubated with different concentrations of nanoparticle-labeled Concanavalin A solutions (ranging from 0 to 1000 nM) according to the typical protocol described above. Figure 4b showed the dose−response curves of ConA on mannose derivatives, Man1, Man4, and Man9, respectively. It was apparent that an increase in Concanavalin A concentration resulted in a corresponding increase in the binding of Concanavalin A to the immobilized carbohydrate spots, as seen from the increase of intensities recorded from the arrayed spots, and saturation of affinities was obtained at a high concentration of Concanavalin A. The surface dissociation constant of Concanavalin A binding with mannose derivatives was estimated from saturation binding experiments and fit to a Langmuir binding isotherm,

$$F = F_{max}[P]/(K_{D,surface} + [P]) \quad (1)$$

where F_{max} is the maximum scanometric signal intensity, a measure of active carbohydrate on the surface, [P] is the total

(34) Liang, P. H.; Wang, S. K.; Wong, C. H. *J. Am. Chem. Soc.* **2007**, *129*, 11177–11184.
(35) Dube, D. H.; Bertozzi, C. R. *Nat. Rev. Drug Discovery* **2005**, *4*, 477–488.
(36) Gambhir, S. S. *Nat. Rev. Cancer* **2002**, *2*, 683–693.

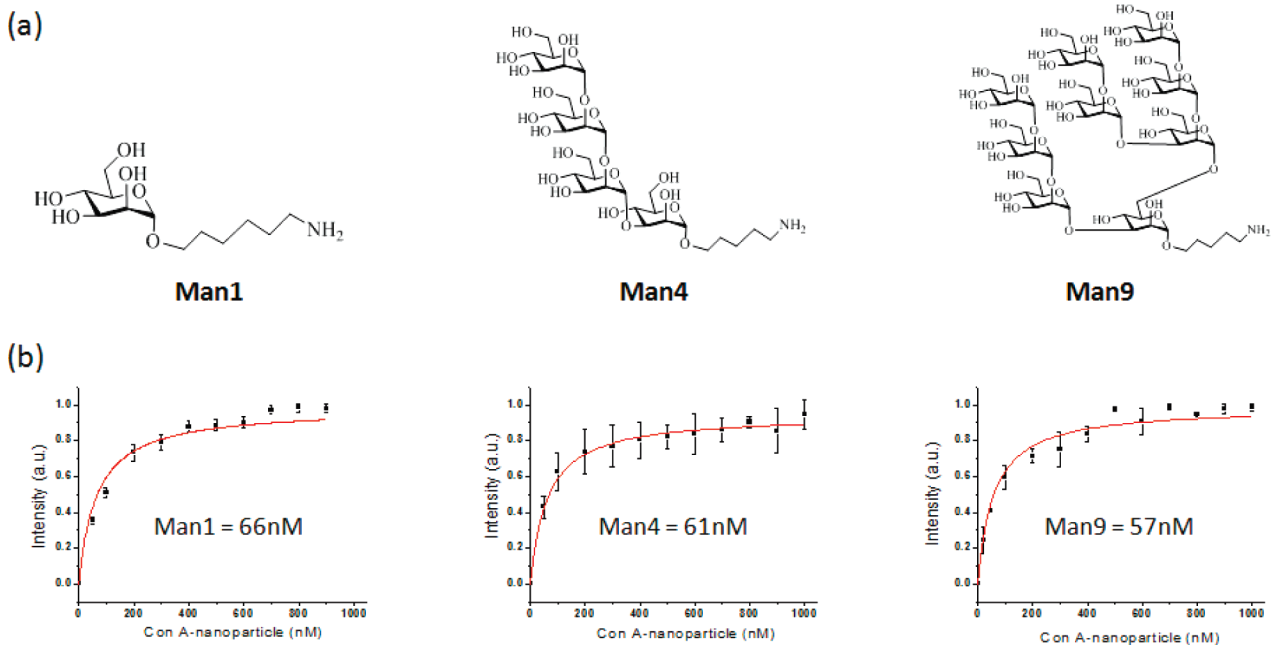

Figure 4. (a) Structures of Man1, Man4, and Man9. (b) The binding curves were obtained from the function of the lectins concentration, and intensity was determined from array images. $K_{D,surface}$ values were obtained by fitting the curves to eq 1. The error bars indicated show the average percentage error for all data points reported.

Con A concentration, and $K_{D,surface}$ is the equilibrium dissociation constant for surface carbohydrate and the Con A protein. The $K_{D,surface}$ values for the binding between Concanavalin A and mannose derivatives were fitted to 66 nM for Man1, 61 nM for Man4, and 57 nM for Man9, respectively. The relative binding affinity of Concanavalin A was Man9 > Man4 > Man1, and this supported that Concanavalin A preferentially binds to a polymannose structure. These results were in good agreement with reported literature and our previous measurements from the fluorescence array.[34,37] The surface dissociation constants obtained in this study confirms that quantitative measurements can accurately study the nature of carbohydrate−protein interaction with the use of a nanoparticle-based assay in a timely and convenient manner.

CONCLUSIONS

We presented a new method for analyzing glycan arrays with an ultrahigh sensitivity using iron oxide/gold core/shell nanoparticle probes and a conventional flatbed scanner. The ultrasensitive detection was achieved by magnetic preconcentration combined with signal amplification. The signal was amplified on the basis of the nanoparticle-promoted reduction of silver, and the sensitivity of this scanometric array detection system exceeded that of the analogous fluorophore system by 1 order of magnitude. The assay also showed excellent specificity to recognize the tumor-associated glycans, SSEA-3, among Globo H and its analogs. In addition, quantitative analysis of binding affinity of carbohydrate−protein interaction on the surface was performed by this assay which is a useful parameter for carbohydrate epitope prediction approaches. In summary, the core−shell nanoparticle assay was a promising analytical method in carbohydrate analysis with the advantages of decreased sampling volume, improved test sensitivity, and reduced cost as compared to fluorescence-based assays. In clinical applications, this ultrasensitive assay for detecting low levels of cancer-associated carbohydrate antigens can be a powerful diagnostic tool for early diagnosis of diseases.

ACKNOWLEDGMENT

This work was supported by Academia Sinica, Taiwan, and National Science Council, Taiwan. (Grant # NSC 97-2113-M-001-009-MY2 to C.-Y.W.)

SUPPORTING INFORMATION AVAILABLE

TEM images, UV−visible spectra, and images of the magnetic test of the iron oxide/gold core/shell nanoparticles and the role of ionic strength on iron oxide/gold nanoparticle−Con A binding. This material is available free of charge via the Internet at http://pubs.acs.org.

Received for review June 5, 2009. Accepted August 5, 2009.

AC9012286

(37) Smith, E. A.; Thomas, W. D.; Kiessling, L. L.; Corn, R. M. *J. Am. Chem. Soc.* **2003**, *125*, 6140–6148.